ASTM INTERNATIONAL

Geotechnical Testing Journal

Mehrad Kamalzare,[1] Thomas F. Zimmie,[2] Barbara Cutler,[3] and W. Randolph Franklin[4]

DOI: 10.1520/GTJ20140226

New Visualization Method to Evaluate Erosion Quantity and Pattern

VOL. 39 / NO. 3 / MAY 2016

Geotechnical Testing Journal

doi:10.1520/GTJ20140226 / Vol. 39 / No. 3 / May 2016 / available online at www.astm.org

Mehrad Kamalzare,[1] Thomas F. Zimmie,[2] Barbara Cutler,[3] and W. Randolph Franklin[4]

New Visualization Method to Evaluate Erosion Quantity and Pattern

Reference

Kamalzare, M., Zimmie, T. F., Cutler, B., and Franklin, W. R., "New Visualization Method to Evaluate Erosion Quantity and Pattern," *Geotechnical Testing Journal*, Vol. 39, No. 3, 2016, pp. 1–16, doi:10.1520/GTJ20140226. ISSN 0149-6115

ABSTRACT

The objective of this research is to develop tools that would improve the understanding of the process of levee failure because of erosion and reduce the risk of failure. Hydraulic erosion is a complicated phenomenon and depends on many different parameters. To improve design criteria for levees, embankments, and earthen structures, the development of realistic computer models that can simulate the erosion process is necessary. Verification of these computer simulations, as with any simulation, is a necessity. In this research, a large number of physical levee erosion tests were performed at 1*g* and at high *g*'s using a geotechnical centrifuge. Centrifuge tests were performed to simulate real (prototype) size levees, and thus to obtain a more realistic model. The erosion was modeled physically in detail. Conventional three-dimensional scanning was used to precisely verify the calculated dimensions of initial and final computer model geometries, but did not yield interim data or measurements of the quantity of eroded soil during the tests. A Kinect device was used to scan and evaluate the volume of eroded soil and variation of the shape of the channels as a function of time. Three-dimensional images were obtained, and variations of different parameters were plotted. Various quantities were measured as a function of time. Based on recorded videos and pictures taken during the tests, it was discovered that the Kinect results agreed well with the physical models. The Kinect is a low-cost sensor, and enables the measurement of the rate of soil erosion, which, if done at all, usually requires expensive equipment. The Kinect device was also used in the centrifuge experiments, and functioned well in the high *g* environment. It is believed to be the first use of a Kinect device in a centrifuge. The application of this method in other laboratory experiments was also investigated.

Keywords

visualization, erosion, soil transportation, overtopping, embankment, geotechnical centrifuge

Manuscript received September 25, 2014; accepted for publication November 12, 2015; published online xx xx xxxx.

[1] Civil and Environmental Engineering Dept., Rensselaer Polytechnic Institute, Troy, NY 12180, United States of America (Corresponding author), e-mail: kamalmrpi@gmail.com; kamalm@rpi.edu

[2] Civil and Environmental Engineering Dept., Rensselaer Polytechnic Institute, Troy, NY 12180, United States of America, e-mail: zimmit@rpi.edu

[3] Computer Science Dept., Rensselaer Polytechnic Institute, Troy, NY 12180, United States of America, e-mail: cutler@cs.rpi.edu

[4] Electrical, Computer, and Systems Engineering Dept., Rensselaer Polytechnic Institute, Troy, NY 12180, United States of America, e-mail: mail@wrfranklin.org

Introduction

Most geotechnical physical modeling facilities feature a system of image capture and analysis to provide measurements of deformation fields. This paper aims to describe a new technique developed for identifying and characterizing the soil hydraulic erosion process of levees, earthen dams, embankments, and similar structures caused by overtopping incidents. Evaluations have been done for levee overtopping erosion tests performed at 1*g* and higher *g* level (centrifuge) conditions but are also applicable in other experiments with different environments. The new technique includes various advances beyond the state-of-the-art described previously. With the use of a new and improved apparatus and software systems, improved measurement performance was achieved. This method provides the capability to measure quantities that were not easy and sometimes impossible to measure previously. This method results in a step forward in measurement utility: small particle-scale transportation features can be detected, allowing soil deformation and erosion patterns to be quantified as a function of time. The proposed methodologies can also be used for other experiments.

During recent decades, there have been continuing efforts to study dam-break hydraulics, including numerical and experimental investigations of dam-break flows and the potential damage caused by the flows. This is understandable because real-time field measurements are extremely difficult to obtain. In fact, numerical simulations play an ever-important role for dam-break flow problems. The erosion process is dependent on several parameters such as soil fines and clay size content, plasticity, and dispersivity, compaction water content, density and degree of saturation, clay mineralogy, and possibly the presence of cementing materials such as iron oxides. Considering all of these parameters, it is very difficult to understand and numerically model the erosion phenomena. Validation of these numerical simulations is also a very challenging task. To provide associated guidance for more rational designs, there is a need for methods that can visualize and evaluate different phases of erosion in laboratory experiments.

Some studies have focused on soil classification. Using an erosion function apparatus (EFA), Briaud et al. (2008) investigated the erodibility of several different types of soil. The soils are classified into different categories of erodibility based on degree of compaction, erosion rate, water velocity, and hydraulic shear stress. Dean et al. (2010) applied experimental steady-state results for different ranges of overtopping. Laboratory results consisting of velocities and durations for acceptable landside levee erosion because of steady flows were examined to determine the physical basis for the erosion. Three bases are examined: (1) velocity above a threshold value, (2) shear stress above a threshold value, and (3) work done on the landside of the levee above a threshold value. The work basis provides the best agreement with the data and a threshold work value, and a work index representing the summation of the product of work above the threshold and time were developed.

Recent research has used effective methods to investigate levee erodibility. Kamalzare et al. (2011) performed a number of laboratory tests on levees with different geometries, and investigated the effects of different parameters on levee erodibility. The rilling process occurring on the landside slope was studied, and erosion effects occurring on the waterside slope were not considered. The duration of various erosion phases were measured, but no data was collected regarding the quantity of eroded soil. Stanier and White (2013) describe a new apparatus and techniques for performing deformation measurements using particle-image velocimetry in the centrifuge environment. The new system includes camera, lighting, and control equipment that facilitates image capture at least 30 times faster than that in legacy systems. Methods for optimizing the addition of artificial seeding on the exposed plane of a geotechnical model were used. These techniques ensured that the precision of the deformation calculations were optimized even in models with multiple soil layers. An example application of a flat footing penetrating sand overlying clay was used to illustrate the performance of the equipment and the artificial seeding optimization technique. Analyses highlight not only the benefits of the new technology, but also the need for carefully optimized experimental procedures to maximize the measurement precision. Dong and Selvadurai (2006) presented a color-visualization-based image-processing technique for the quantitative determination of a chemical dye concentration in a fluid-saturated porous column composed of glass beads. In this image-processing technique, an image filter is designed by taking into account the porous structure of the medium and color characteristics of both the fluid and the solid particles to extract the color representation of the dye solution in pore space, which enables the image quantification. A comparison of experimental results with analytical and numerical simulations illustrates the efficiency and accuracy of the image-processing method for determining the chemical concentrations in the porous medium.

Iskander et al. (1994) demonstrated the feasibility of producing transparent materials, which exhibit macroscopic properties representative of the geotechnical properties of natural soils. The transparent "soils" discussed are made by consolidating suspensions of amorphous silica in liquids with matching optical refractive indices. The measured shear strengths and permeabilities of the transparent soils are characteristic of natural clays and silts. Lo et al. (2010) proposed a new water-based transparent material called "Aquabeads" for modeling flow in natural soils. Three types of this material were used to model miscible and multiphase flow-transport processes in layered soil systems. An optical system was set up to trace flow movements in a two-dimensional (2D) physical model of a soil profile, and

analyzed using digital image processing to define images of 2D concentration profiles in the model. Model surfactant flushing tests were conducted using a layered soil system and two contaminants, mineral oil and motor oil, to illustrate the feasibility of using this water-based polymer to visualize geoenvironmental contamination problems. Because a transparent soil was used, the optical systems allow for visualizing surfactant flushing. The study demonstrates that Aquabeads are suitable for modeling multiphase flow, particularly in educational settings. Kamalzare et al. (2013a, 2013b), Kamalzare et al. (2012a, 2012b), Holmes et al. (2011), Stuetzle et al. (2011), Yu et al. (2009), and Xiao et al. (2009) also apply different numerical techniques to study and simulate various aspects of the erosion phenomena.

Raschke and Hryciw (1997) present a semi-automated technique for obtaining the grain-size distribution (GSD) of granular soils using computer vision. Backlighted digital images of a soil specimen dispersed over a glass specimen plate are acquired at three different magnifications. Images of the specimen were acquired by placing the specimen plate randomly beneath the field of view of a charged coupled device (CCD) video camera. The size of particles with projected areas from 50 to 2000 px^2 was measured in each image. Multiple images were acquired at each magnification until the measured size distribution of particles counted at that magnification stabilized. Probabilistic corrections were then used to obtain a statistically unbiased GSD from the image data obtained at all three magnifications. A comparison of GSD data for two uniform and two non-uniform soils using both computer vision and sieving was also presented.

Although much work has been done to simulate erosion in the field of computer graphics, there has been limited validation. This is mostly because of limitations of current laboratory measurement methods. A primary objective of this research was to find a methodology to validate computer simulations by laboratory experimentation. Therefore, in this research, laboratory tests using model levees have been performed to improve the computer simulations of levee and embankment erosion. To evaluate the effects of water flow on real levees, some centrifuge tests were also performed simulating full-scale prototype levees and embankments. A new visualization methodology has been introduced that not only provides 3D images of erosion channels but also the capability to validate the quantity of the erosion and the evolution of erosion channels as a function of time.

Conventional Visualization Methods

Techniques for the measurement of deformations and soil transport in geotechnical models have developed significantly in recent years. Early studies by Butterfield et al. (1970) and Andrawes and Butterfield (1973) reported the use of stereo photogrammetry, in which individual particle movements as seen in stereo pair photographs, were measured manually. The recent introduction of digital technology has removed the need for painstaking manual film measurements. The technique of PIV (also known as digital image correlation) has been widely applied across many branches of engineering (Raffel et al. 2007; Pan et al. 2009; Sutton et al. 2009). The use of PIV and photogrammetry to measure soil displacement in small-scale physical models has led to a significant increase in measurement accuracy and precision relative to previously utilized techniques (White et al. 2003). Furthermore, the number of measurement points available in the analysis process has become a function of discretization (patch size) rather than the number of identifiable features (e.g., target markers) on an exposed plane of the model (Stanier and White 2013).

THREE-DIMENSIONAL (3D) LASER RANGE SCANNER (LIDAR)

The other conventional and widely used visualization method for both outdoor large-scale and indoor small-scale experiments is laser scanning. Three-dimensional object scanning allows enhancement of the design process, speeds up and reduces data-collection errors, saves time and money, and thus makes an attractive alternative to traditional data-collection techniques. 3D scanning is also used for mobile mapping, surveying, scanning of buildings and building interiors, and in archaeology. Lidar is a remote-sensing technology that measures distance by illuminating a target with a laser and analyzing the reflected light. Lidar was developed in the early 1960s, shortly after the invention of the laser, and combined laser's focused imaging with radar's ability to calculate distances by measuring the time for the signal to return (Goyer and Watson 1963). Lidar uses ultraviolet, visible, or near infrared light to image objects and can be used with a wide range of targets, including non-metallic objects, rocks, rain, chemical compounds, aerosols, clouds, and even single molecules.

In our research, the initial and final surface geometries of the model levee for different overtopping erosion experiments were recorded using a 3D laser range scanner (Lidar) and were analyzed using the data structure developed in this study. The acquired surface data from each test could then be used to further visualize the final results of the physical overtopping simulations. The laser range scanner rotated through a user-specified angle and, using a single laser beam, conducted a scan of the surface at each incremental rotation within the range of rotation. Each incremental movement was characterized by a new pulse of the laser beam that collected data based on features in surface elevation or geometry of the object of interest at that specific position being scanned. The laser range scanner used in this research was a Leica 30 HDS 3000, by Leica Geosystems HDS, LLC. The laser range scanner is shown in **Fig. 1**.

To facilitate the recognition of the boundaries of the model levee, brightly colored tape was placed on the edges of the top

J_ID: GTJ DOI: 10.1520/GTJ20140226 Date: 25-January-16 Stage: Page: 4 Total Pages: 17

FIG. 1 Leica HDS 3000 laser range scanner.

of the model box in irregular patterns. The purpose for the irregular patterns of the tape was to differentiate the orientation of the model box. For each physical simulation, there were four total scans associated with each test; two scans, one from each side of the model levee were obtained so that a scan of the entire surface could be obtained by the scanner. Two initial scans were obtained following the completion of construction of the model levee, but prior to turning on the flow of water. The first scan featured the model box oriented with the landside of the levee toward the scanner. Once scanning was completed, the model was rotated 180° so that the waterside of the levee was oriented toward the scanner and the second scan began. The same scanning procedure was done within 5 to 10 min following completion of the physical erosion test on the levee model.

The presence of the model box walls partially obstructed the scan, making a rotation necessary. The two scans of the same surface were aligned and overlaid on top of one another during the data processing. However, because the Lidar scanner is more mobile than the experimental setup, for some of the experiments, the scanner was moved around the room to acquire data from different angles, while the location of the model box was kept fixed during the whole experiment. From any one angle, it is impossible to see all of the surface data, and it is necessary to perform scans from different angles. Therefore, there were six total scans associated with each test in this method. Following completion of construction of the model levee, but prior to water flow, three initial scans were done. This was necessary because the location of the Lidar was changed after each scan; three scans were required to make a full 3D image of the room. The same scanning procedure was done immediately after completion of the physical erosion test on the levee model.

Layer surface data was collected in the form of a point cloud via a 3D laser range scanner. This 3D point data was then run through a data-preparation script that, for each scan, registered the points. It was then aligned to a regular grid in the XY plane, retaining the height values of the points. The points in a grid space used averaged heights to acquire a single value for use in the data structure. If there were multiple soil layers in a single model, this procedure was repeated for each layer (as they were being assembled), generating a layered data structure. The end result was a grid in which each cell contains an array of soil layers with heights and depths. The whole room was scanned from each angle. The model levee was then cropped out of the picture in the next step to find a high-resolution image showing the surface of the levee.

Fig. 2 shows a schematic drawing of elevation and plan view of a typical experimental setup. Different drainage systems were used based on the water flow and the type of the soil (Kamalzare et al. 2013a). The grain size distribution of the soil was determined according to ASTM D6913-04 (2009). Several tests were performed and the average of the results is presented in **Fig. 3**. The soil is classified as "SC" according to the Unified Soil Classification System (USCS). Other characteristics of the soil are shown in **Table 1**.

From each of the cardinal directions surrounding the experiment, a fine resolution scan was taken to obtain as much surface detail as possible. This scan usually had 1 mm resolution. From at least two perspectives, a coarse resolution scan (10 mm) was taken of the entire room. The coarse resolution scans were used to add key points necessary to transform the data into the same coordinate system. From the fine resolution scans, the surface points were cropped out. They were then axis-aligned and converted into a data format recognizable by the erosion simulation. The collected scan data, which was processed digitally, yielded the visualized representation of the data shown in **Fig. 4**.

The variation of color in the visualization represents different elevations of the model levee. Eroded areas are readily seen by the integration of one color in another (i.e., the yellow in the orange colored area).

COMPUTER SIMULATION

During the course of this research, a computer simulation was also developed to model hydraulic soil erosion (Stuetzle 2012; Kamalzare 2013). To model the levee system, the high-resolution particle-based Lagrangian method based on smoothed particle hydrodynamics (SPHs) was used. This method was first presented by Gingold and Monaghan (1977), and is based on the Navier–Stokes equations and discretized

J_ID: GTJ DOI: 10.1520/GTJ20140226 Date: 25-January-16 Stage: Page: 5 Total Pages: 17

FIG. 2

Schematic drawing of elevation and plan view of a typical experimental setup.

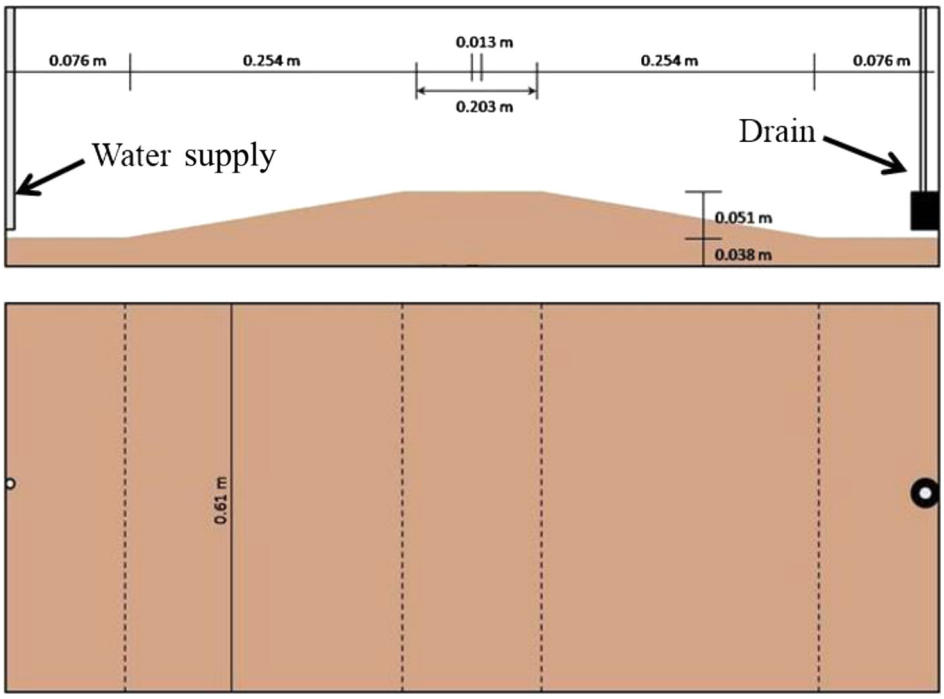

FIG. 3 Grain size distribution of the soil.

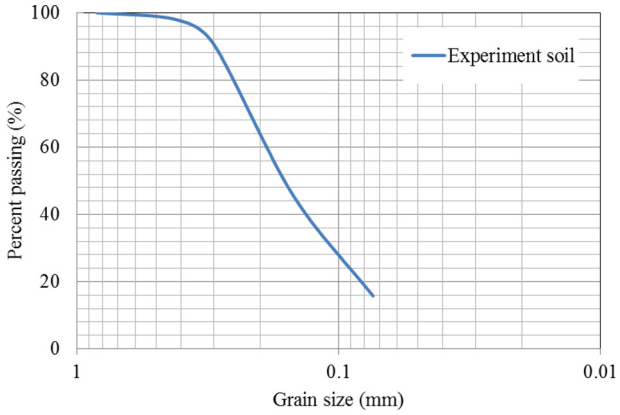

TABLE 1 Soil characteristics.

Property	Numerical Value
D_{10} (mm)	0.074
D_{30} (mm)	0.11
D_{60} (mm)	0.19
Coefficient of uniformity	2.57
Coefficient of curvature	0.86
Liquid limit	17
Plastic limit	11

into a set of particles. The solution is based on momentum and mass conservation equations. To model the soil, a set of statically placed erodible particles was used. Three types of particles were introduced in the simulation: soil particles, boundary particles (soil particles near a water particle), and water particles. A large number of laboratory experiments were performed in both 1*g* and higher *g* level (centrifuge) conditions to evaluate the appropriate coefficients that were critical to define the relationships between different particles in the computer model. For each of the simulations, approximately 450,000 water and

FIG. 4 Visualization of an overtopping erosion experiment.

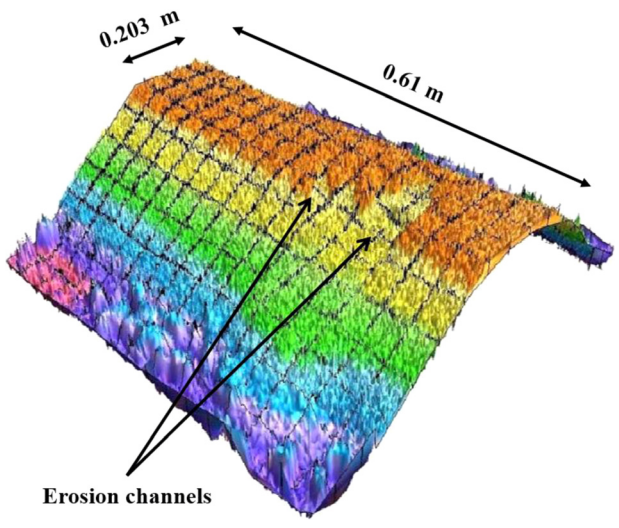

J_ID: GTJ DOI: 10.1520/GTJ20140226 Date: 25-January-16 Stage: Page: 6 Total Pages: 17

2,500,000 soil particles were introduced. The results of computer simulations for one of the experiments are shown in **Fig. 5** as an example.

To validate the computer simulations, a comparison was performed between the digital simulations at different stages of overtopping, and the actual physical experiments performed in the laboratory. The results of Lidar 3D visualizations were used for the comparison, and a good match was observed between the overall qualities of the erosion channels. However, to determine the accuracy of the computer model, it was necessary to verify the amount of soil eroded in each digital simulation. The amount of eroded soil can be calculated as a function of time in the computer model, but it is a challenge to measure the rate of eroding soil in the physical erosion experiments. At the same time, the Lidar scanning is a time-consuming procedure. Depending on the size of the model, each scanning would take about 10 min, which makes it impossible to record quick incidents. In the case of erosion experiments, it was not feasible to scan and record the surface of the levee during the test, and only the initial and final surfaces were recorded. Therefore, the progression of erosion could not be measured. Also, the Lidar cannot be used in centrifuge experiments. One of the main objectives of this research was to find a method to measure the volume of eroded soil and the shape of the formed rills with respect to the time of overtopping. In the next section, a new visualization methodology is introduced, which enables the measurement of the quantity of erosion as a function of time. This method was also utilized in the centrifuge experiments. To the best of our knowledge, this is the first time that this visualization methodology has been applied to the study of erosion.

FIG. 5 Digital simulations for different stages of overtopping (*a*) before overtopping, (*b*) during overtopping, and (*c*) full breach.

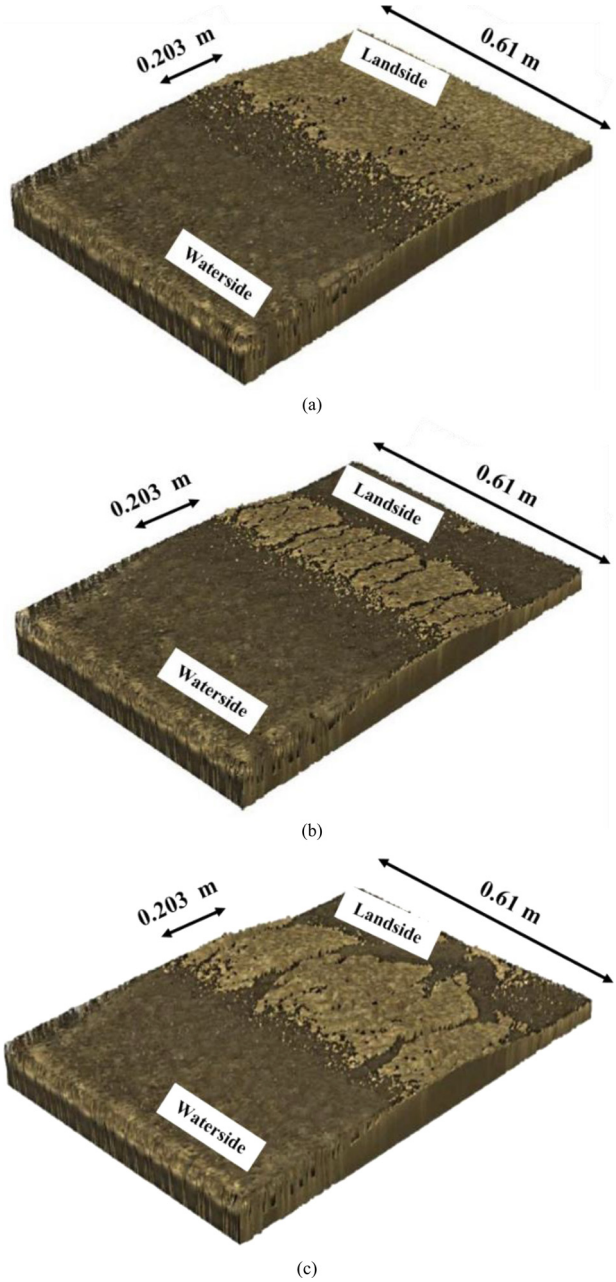

A Visualization Method to Measure Erosion Quantity and Evolution

Because of the limitation of current experimental methods, it is quite difficult if not impossible to measure the exact amount of transported soil and the erosion evolution during hydraulic erosion experiments. However, the process of channel formation during an overtopping experiment was recorded with a Kinect sensor. Unlike a regular camera or even a high-speed camera, the Kinect sensor records additional information regarding elevations and depths of different parts of the channels. The Kinect sensor is part of a Microsoft gaming system, and because of the economics of mass production, can be typically purchased for about $100.00. The technical capabilities of the Kinect system can be duplicated in a custom design, but the cost will be several thousand dollars. A brief introduction about the Kinect sensor (Xbox 360, by Microsoft) is presented below, followed by details of the methodology. This paper and associated research is neither an endorsement nor promotion for the Kinect system.

KINECT SENSOR

The Kinect sensor is a horizontal bar connected to a small, motorized base and is designed to be positioned lengthwise above or below the video display. The device has an RGB camera that delivers the three basic color components (red, green, and blue) on three different wires. It also has a depth sensor and two multi-array microphones. It provides full-body 3D motion capture, facial recognition, and voice-recognition capabilities (**Fig. 6**). The depth sensor consists of an infrared laser projector combined with a monochrome complementary metal-oxide semiconductor (CMOS) sensor, which captures video data in 3D under any light conditions. The sensing range of the

J_ID: GTJ DOI: 10.1520/GTJ20140226 Date: 25-January-16 Stage: Page: 7 Total Pages: 17

FIG. 6 Kinect sensor.

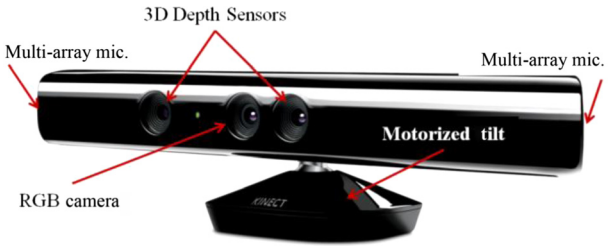

depth sensor is adjustable, and the Kinect software is capable of automatically calibrating the sensor based on the object and its physical environment, accommodating the presence of any obstacles.

Reverse engineering has determined that the Kinect is able to record video at a frame rate of almost 9 Hz to 30 Hz, depending on resolution. The default video stream uses 8-bit video graphics array (VGA) resolution (640 × 480 pixels), but the hardware is capable of resolutions up to 1280 × 1024 (at a lower frame rate) and different color formats. The monochrome depth-sensing video stream is in VGA resolution (640 × 480 pixels) with 11-bit depth, which provides 2048 levels of sensitivity. The Kinect can also stream the view from its infrared (IR) camera directly, before it has been converted into a depth map, as 640 × 480 video or 1280 × 1024 at a lower frame rate. The Kinect sensor has a practical ranging limit of 1.2–3.5 m distance; however, the sensor can maintain tracking through an extended range of approximately 0.7–6 m. The sensor has an angular field of view of 57° horizontally and 43° vertically, while the motorized pivot is capable of tilting the sensor up to 27° either up or down. The horizontal field of the Kinect sensor at the minimum viewing distance of almost 0.8 m is, therefore, 87 cm, and the vertical field is 63 cm, resulting in a resolution of over 1.3 mm per pixel. **Table 2** summarizes the technical properties of the Kinect sensor.

APPLICATION OF THE KINECT SENSOR IN OVERTOPPING EXPERIMENTS

Considering the dimensions of the modeled levees and the Kinect viewing angle, a minimum distance of 1.3 m was required to visualize the whole model. This distance was measured from the highest point of the modeled levee to the Kinect, and is consistent with the practical ranging limit of 1.2–3.5 m for the depth sensor. In 1*g* experiments, the Kinect was connected to a vertical metal bar, and secured to a table placed in the middle of the room. An important consideration for setting up the Kinect prior to experiments is to place the sensor on a stable surface in a location where it will not fall or be struck during use. It should also be accurately leveled, otherwise there will be errors in the recorded depth, and a complicated and time-consuming process is needed to cancel this error.

TABLE 2 Technical details of the Kinect sensor.

Property	Description
Sensor	Color and depth-sensing lenses Voice microphone array Tilt motor for sensor adjustment
Field of view	Horizontal field of view: 57° Vertical field of view: 43° Physical tilt range: 27° Depth sensor range: 1.2 m–3.5 m
Data streams	320 × 240 16-bit depth at 30 frames/s 640 × 480 32-bit color at 30 frames/s 16-kHz, 24-bit mono pulse code
Skeletal tracking system	Tracks up to six people, including two active players Tracks 20 joints per active player

After placing the Kinect at the desired distance above the model and leveling, its position was fixed. The Kinect was connected to a laptop with a USB port, which controlled the Kinect, and saved all measured data acquired during the experiment. To minimize noise, it is important to not place the Kinect on or in front of any surface that vibrates or makes noise (e.g., speakers). It should also be kept out of direct sunlight. It should be used within its specified operating temperature range of 5°C to 35°C.

The lighting of the room that the experiment is being performed in should be considered. The room should have sufficient light so that the model is clearly visible and evenly lit. Some lighting conditions make it difficult for Kinect to identify the objects and track their movements. In general, incandescent, fluorescent, and natural lighting work well.

The depth sensor reads depth information from reflected light. Objects that are highly reflective, such as shiny metals or highly absorptive materials, may not be registered by the depth sensor as successfully as other objects. During experiments performed herein and after adding water to the system, it was important to avoid light reflections.

The Kinect was also used in centrifuge experiments to investigate soil erosion. In centrifuge experiments, forces increase with increased *g* levels, and materials can be subjected to large forces compared to 1*g* tests. Some of the challenges were to ensure that the Kinect would function at high *g* loads and not move during the centrifuge tests. A frame and an extended arm were constructed to secure the Kinect during the centrifuge experiments. The arm attached the Kinect frame to the centrifuge beam. The Kinect was placed as close as possible to the center of the centrifuge to minimize the centrifugal loads. **Fig. 7** shows the Kinect secured with the frame, and placed on the centrifuge prior to an experiment. In a centrifuge experiment, the centrifuge basket rotates and becomes perpendicular to the Kinect. The distance between the highest point of the

FIG. 7 Kinect sensor setup for the centrifuge experiments.

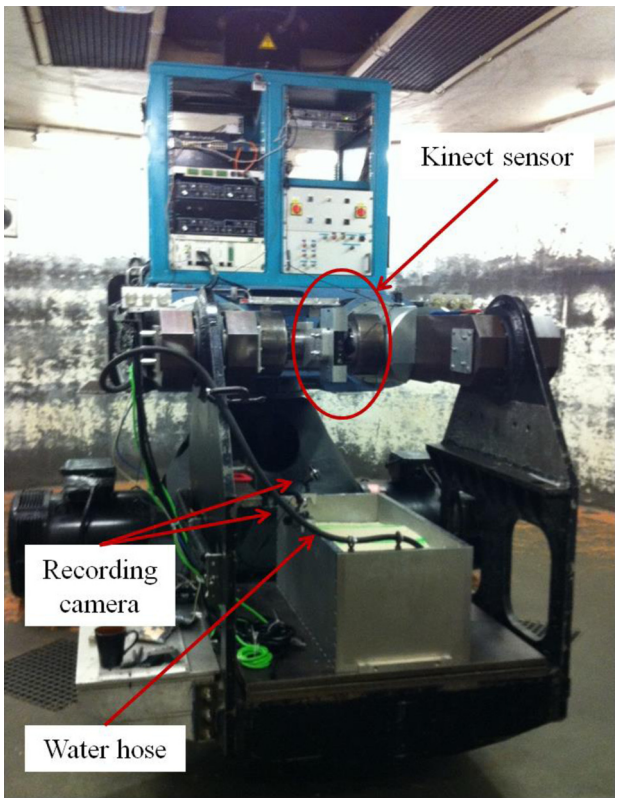

FIG. 8 Illustration of the Kinect resolution and its position.

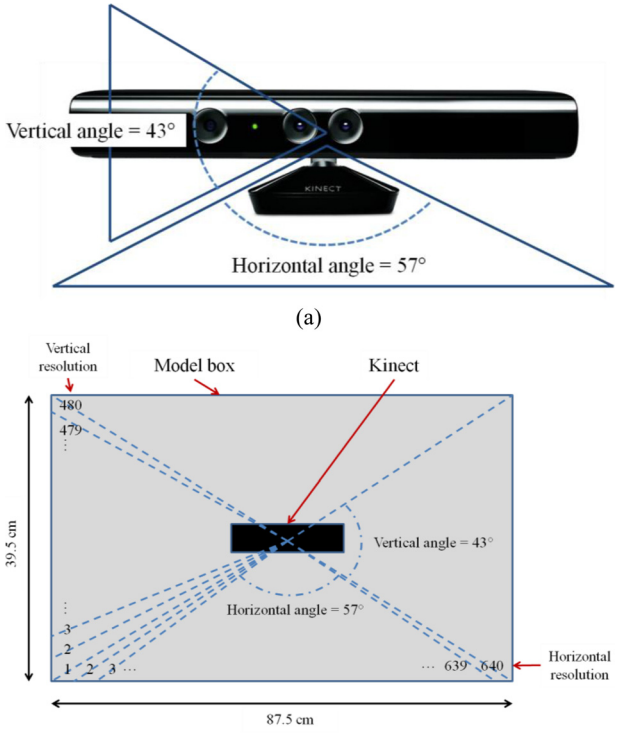

model levee and the Kinect was equal to 1.25 m, which is in the suggested range for Kinect.

Prior to an experiment, the Kinect sensor was calibrated to avoid any unpredicted noise or error. After fixing the position of both the Kinect and the model box for each experiment, a known object was placed on the box. The distance between the Kinect and the known object was then scanned and calculated with the Kinect. The same distance was also measured with a ruler. These two measurements were then compared after the experiment, and any probable differences could be modified in the recorded results.

DATA PROCESSING

As mentioned previously, the Kinect has a horizontal and vertical angle of view equal to 57° and 43°, respectively. It also has a resolution equal to 640 × 480; when the Kinect is placed above the modeled levee, it divides the length of the levee into 640 sections. Similarly, the width of the levee is divided into 480 sections. This results in a grid with a dimension of 640 × 480. Dividing the horizontal view angle, 57°, by the horizontal resolution, 640, yields a horizontal angle equal to 0.0892° for each of the cells in the main grid. Similarly, dividing the vertical view angle, 43°, by the vertical resolution, 480, yields a vertical angle equal to 0.0897° for each of the cells in the main grid. Kinect sees each cell like a pyramid with almost the same horizontal and vertical angles. **Fig. 8(a)** and **8(b)** illustrate the Kinect angles of view and its resolution and position for the laboratory experiments.

Given the length of the modeled levee, the length of each cell in the main grid was calculated by dividing the length of the levee by the horizontal resolution of the Kinect. Similarly, the width of each cell was calculated as in the following:

$$\text{Length of each cell in the grid} = \frac{\text{Length of the levee}}{\text{Horizontal resolution}} = \frac{87.5\,\text{cm}}{640} = 0.1367\,\text{cm} \quad (1)$$

$$\text{Width of each cell in the grid} = \frac{\text{Width of the levee}}{\text{Vertical resolution}} = \frac{39.5\,\text{cm}}{480} = 0.0823\,\text{cm} \quad (2)$$

Therefore, the Kinect sees the surface of the levee as a grid with 307,200 cells, with dimensions calculated above.

Different types of data can be obtained from Kinect sensor scanning. Depth data was of most interest for this research. The resulting data was a large set of numbers, which are actually measured distances between the Kinect and the modeled levee surface for each of the cells. For the erosion experiments, the Kinect was set to record ten frames per second. For a typical experiment, 5000 to 8000 frames were recorded. Each frame contained depth data for 307,200 cells. Because items such as light reflection or a sudden water movement can add noise to

J_ID: GTJ DOI: 10.1520/GTJ20140226 Date: 25-January-16 Stage: Page: 9 Total Pages: 17

the recorded data, the data was averaged over every 10 frames. This minimized recorded noise. Open-source software was used to open and analyze the recorded files.

Because the position of the Kinect and the model levee were fixed during the experiments, the positions of the cells were constant. Considering the size of the particles of the soil used in this research, and the relatively small dimensions of the cells, it can be confidently assumed that the difference between the recorded depths for a cell in two different frames would be equal to the amount of eroded soil in each cell, in the time period between the frames. Thus, the amount of the eroded soil at any specific time during the overtopping experiment can be calculated by subtracting the values of the recorded frame at a given time from the first recorded frame at the beginning of the experiment. The variation of the amount of eroded soil can be calculated at different times, i.e., the volume of eroded soil versus time (erosion rate).

To calculate the amount of eroded soil, the volume of the pyramid, which is between the Kinect and four neighboring cells, was calculated. The amount of eroded soil in the time period between two specific frames would then be equal to the difference between the volumes of the two respective pyramids. The volume of the pyramids can be calculated by calculating the area of the triangles at each side. The area of the triangles can be calculated using Eq 3:

$$\text{Area} = 1/2AB\sin\alpha \tag{3}$$

where:

A and B = the depths (distances) of the first and second cell, respectively, and

α = the cell's angle of the view, which was calculated above (for both vertical and horizontal views is equal to 0.0892°).

Fig. 9 illustrates the details of the calculations in 2D.

Considering the size of the modeled levee, the resolution of the Kinect is relatively high, and the dimensions of the cells are relatively small. Also the frequency of frame recording is relatively high. As noted, the Kinect recorded 10 frames per second (it can be increased to 30 frames per second). Therefore, when calculating the amount of eroded soil in each cell, instead of finding the difference between two pyramids, the difference between two cubes can be calculated. It was reasonable to assume that the recorded depths represented an average of the depth of the total cell area. Thus, each of the recorded depths represents the average depth of a rectangular area on the levee's surface with dimensions equal to $L = 1.3$ mm, and $W = 0.8$ mm. Multiplying the area of each cell (0.01125 cm^2) by the recorded depth of that cell, and finding the difference between these values for a specific cell in two different frames, yields the volume of the eroded soil in that specific cell in the time period between those two frames. In the following sections, the accuracy of the results and the validity of the above assumptions are discussed.

FIG. 9 Calculating the amount of erosion between two frames.

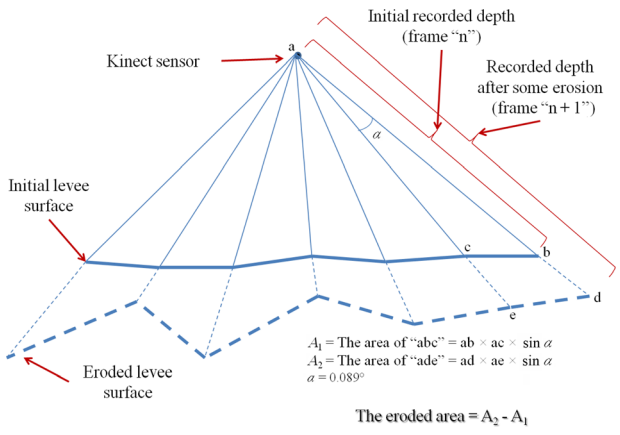

Results and Verification

The process of channel formation during an overtopping experiment was recorded with the Kinect. Unlike a regular camera or even a high-speed camera, the Kinect records additional information regarding elevations and depths of different parts of the channels. Differing depths can be presented using different colors, enabling one to follow the channel-formation process and investigate the erosion process. **Fig. 10(a)–10(d)** shows the results of the Kinect visualization at four different times during one of the overtopping experiments as an example. Each of the figures has been recorded at a different time (t_1, t_2, t_3, and t_4) during the experiment. The sides of the experiment box and different parts of the levee can be seen. The progression of overtopping during the experiment has been clearly recorded and shown in these figures. As the measured depth increases, the coloration proceeds from brown to green. The water overtopped the levee from the waterside, which is on the left, to the landside, which is on the right. Some small channels propagate on the crest of the levee, and eventually the primary channel forms and the levee breaches. In addition to the colors, there are contour lines on each figure that show elevations.

These results can be useful for obtaining an understanding of channel propagation and are used for verifying predicted depths of the channels obtained by digital simulations; however, measurements of the quantity of erosion are required, that is, the volume of eroded soil as a function of time. As mentioned previously, the Kinect sensor meshes the surface of the levee to a rectangular grid, and records the depth of the each cell at different time steps. Theoretically, it should be easy to find the differences between recorded values of the frames, and compute the amount of eroded soil, but there are several challenges to completing this task. Each frame contains information about the location and depth of 307,200 cells. For each experiment, about 5000 to 8000 frames were recorded, resulting in a large amount of data. Obviously, it is necessary to use a computer

J_ID: GTJ DOI: 10.1520/GTJ20140226 Date: 25-January-16 Stage: Page: 10 Total Pages: 17

FIG. 10 Kinect visualization of progression of erosion for a 1*g* overtopping experiment (plan view) $t_1 < t_2 < t_3 < t_4$.

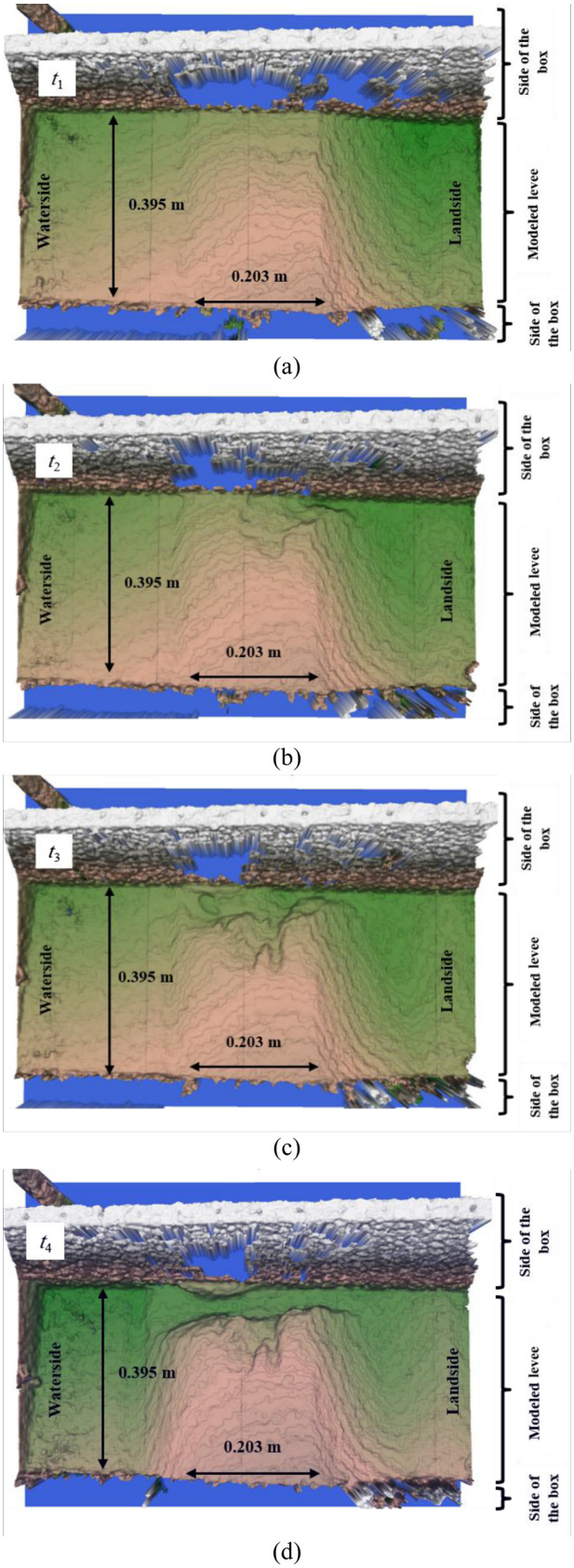

code to handle the data. Another challenge is noise in the data. Some noise can be explained because of movement of the water during the experiment, and consequently reflection. The nature of this type of noise is random, and random noise is challenging because it is not similar to regular noise that can be easily filtered. Analyzed results of measured depths for a centrifuge experiment are presented in **Fig. 11** as an example. Images at different times during the test were analyzed and produced, but, in this figure, only the levee after full breach has been shown. No effort has been made to reduce the noise in these images. As mentioned earlier, the Kinect was placed on top of the experiment box to be able to capture the whole modeled levee during the experiment. However, in addition to the plan view of the levee, the sides of the experiment box could also be seen in all of the Kinect videos and images. This would help to distinguish the borders of the modeled levee in early stages of the processing of the recorded images. The sides of the box would be deleted from the images during final stage of the analyses of depth measurement.

To eliminate the noisy data, two new computer codes were generated. One located the noise and filtered it out of the recorded data, and the information in a frame was first copied in a 640 × 480 matrix. The standard deviation of the values in the matrix was then calculated, indicating the amount of variation or dispersion existing from the average (mean) value. In the next step, each of the values in the matrix was compared to the calculated standard deviation, and if the difference was larger than 10 cm, the data was considered noise. The noise was then eliminated from the matrix. The time step between two

FIG. 11 Analyzed results of Kinect for measuring depth of erosion for a centrifuge experiment after full breach (plan view).

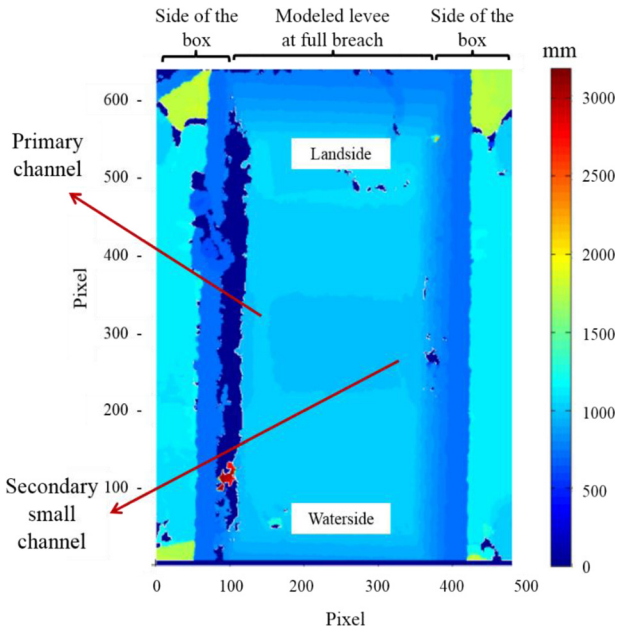

J_ID: GTJ DOI: 10.1520/GTJ20140226 Date: 25-January-16 Stage: Page: 11 Total Pages: 17

successive frames is only 0.1 s. Based on the results and observations of previous experiments, it is clear that it is impossible for any part of the levee to erode 10 cm in such a short time.

The second computer code was intended to calculate the amount of erosion. However, even after noise reduction, it was required to eliminate some data from the system. These data were from different parts of the box, or other external objects that were in the Kinect view field. After calculating the difference between the two frames, the data was cropped in a manner so that only information regarding the primary erosion channel remained. All the values in the difference matrix were then added and the amount of eroded soil in the main channel was calculated. Repeating the above procedure resulted in the values of erosion in the primary erosion channel as a function of time. **Fig. 12(a)** and **12(b)** shows the results of the measured depths for the same centrifuge experiment and at the same time (full breach) as shown in **Fig. 11** after execution of each of the computer codes.

It is important to mount the Kinect so that only the experiment model is placed in the Kinect view field, and eliminate other objects from the view of the Kinect as much as possible. The noise reduction process described above is much more efficient if the Kinect only sees the model, and no other object.

The eroded channels could also be plotted in 3D space. Images were plotted viewed from different angles and the intensity of the erosion at different parts of the main channel was studied. This was helpful for observing and investigating the effects of erosion on the shape of the channels. As an example, the 3D view of the main channel of the same centrifuge experiment is shown in **Fig. 13**. It should be noted that only part of the levee has been shown in this figure (the primary channel and the areas with major erosion). The areas with no erosion or very minor erosion have been cropped out during the noise-reduction procedures.

The computer codes not only provided different images and information about the shape of the channels, but also calculated the quantity of erosion. However, because some assumptions were made in the process of analyzing the Kinect data, it was necessary to validate the data. For this purpose, the recorded video of the high-speed camera was used to provide images of the levee breach using 12-s intervals. The primary channel was scaled, and its width, length, and depth measured. The amount of eroded soil during that interval was calculated manually by scaling the video images and measuring the width and depth of different erosion sections and channels. These values were compared to the results of the Kinect data. Dimensions were measured and scaled carefully. However, there are inherent errors because of limited angle of view of the high-speed camera, and the length of the model levee. It is estimated that the measured values of depth and length are subject to about 10 % error. The authors feel the accuracy estimate of 10 % is likely a conservative number. Volume measurements on objects

FIG. 12 Results of analyses on the measured depths for a centrifuge experiment at full breach (plan view): (a) after noise-reduction procedure (first computer code), and (b) after cropping the primary channel (second computer code).

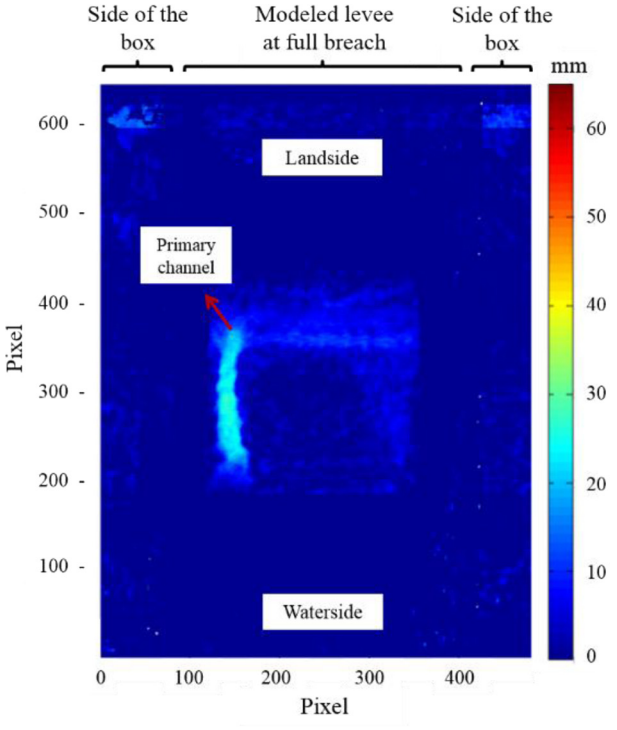

J_ID: GTJ DOI: 10.1520/GTJ20140226 Date: 25-January-16 Stage: Page: 12 Total Pages: 17

FIG. 13

Three-dimensional view of the primary channel in a centrifuge experiment (at full breach).

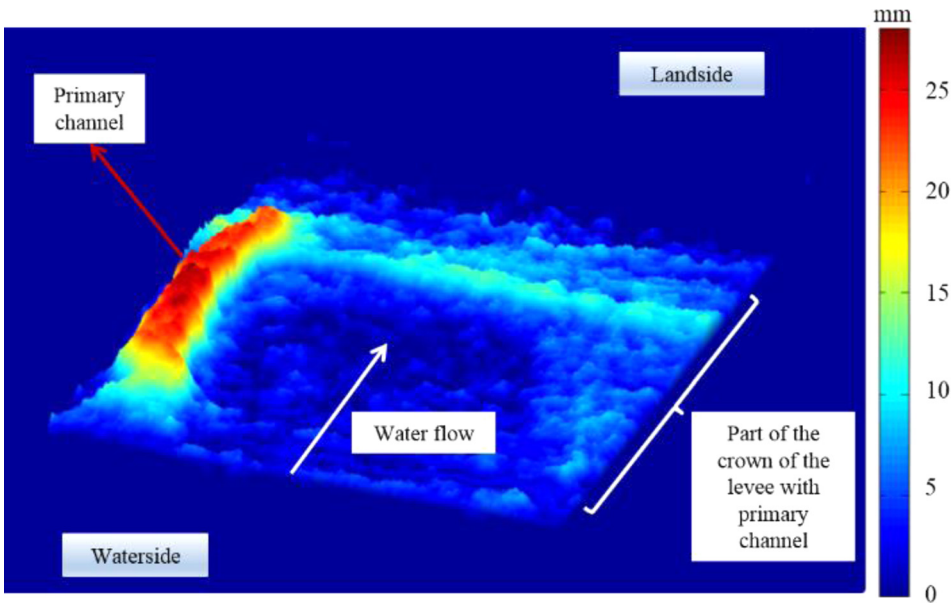

with well-defined boundaries, such as wooden blocks, and metal cylinders agree within a few % of Kinect determinations. However volume measurements on objects with rough boundaries like soil are less accurate, but still are accurate within 10 %. As an example, the calculated erosion volumes for two different centrifuge experiments are plotted in two graphs and shown in **Fig. 14** in comparison to the values for the same experiment, calculated from the Kinect data.

One can observe three different slopes, which are related to different erosion phases of the experiments in both graphs shown in **Fig. 14**. Each blue point on the graph shows the amount of erosion based on the analyses of the recorded Kinect data. For example, looking at **Fig. 14(b)**, the difference between the first recorded frame in the experiment CMBL-04 at time equal to 8.5 min, and the frame that was recorded at time equal to 13 min would be equal to the amount of the erosion that has occurred in that 4.5-min time period. This has been shown with a blue point at time equal to 13 min on the graph. It is important to record the first frame prior to adding water to the system. This would create a reference for calculations regarding the initial situation of the levee with no erosion. The results are quite comparable, indicating the assumptions utilized in analyses of the Kinect data appear reasonable. It also indicates the Kinect data appears to be quite acceptable. It should be noted that the speed of surface erosion should theoretically scale with g^2 because the model is smaller and gravity is larger, both by factors of g.

The extent to which this actually happens is a topic for future study. The research reported in this paper focuses on the nature of the erosion, rather than on its speed. There is insufficient data to validate the g^2 scaling relation for erosion time.

FIG. 14 Comparison between the measured values of erosion and the values calculated with the computers codes from the Kinect data (a) centrifuge experiment CMBL-03, and (b) centrifuge experiment CMBL-04.

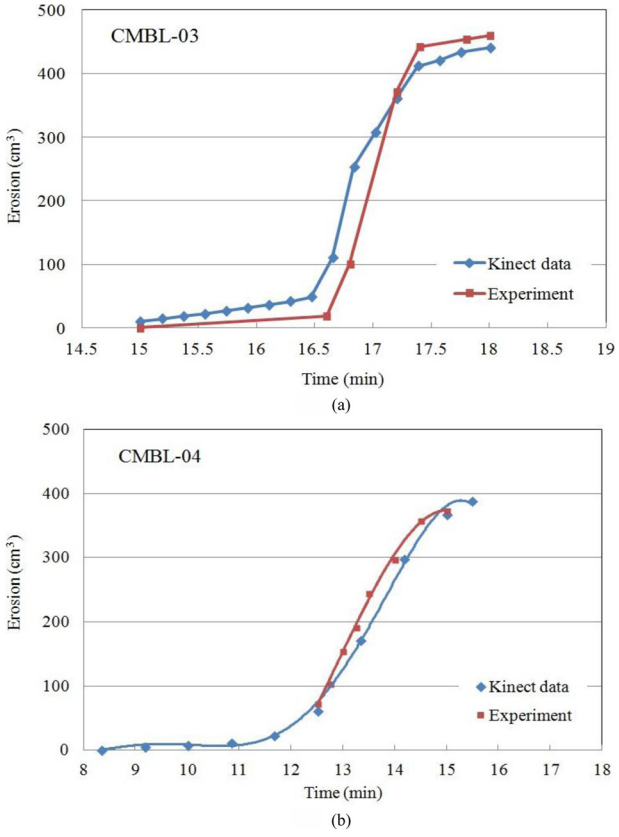

J_ID: GTJ DOI: 10.1520/GTJ20140226 Date: 25-January-16 Stage: Page: 13 Total Pages: 17

FIG. 15

Formation of the primary channel in experiment CMBL-04 (plan view).

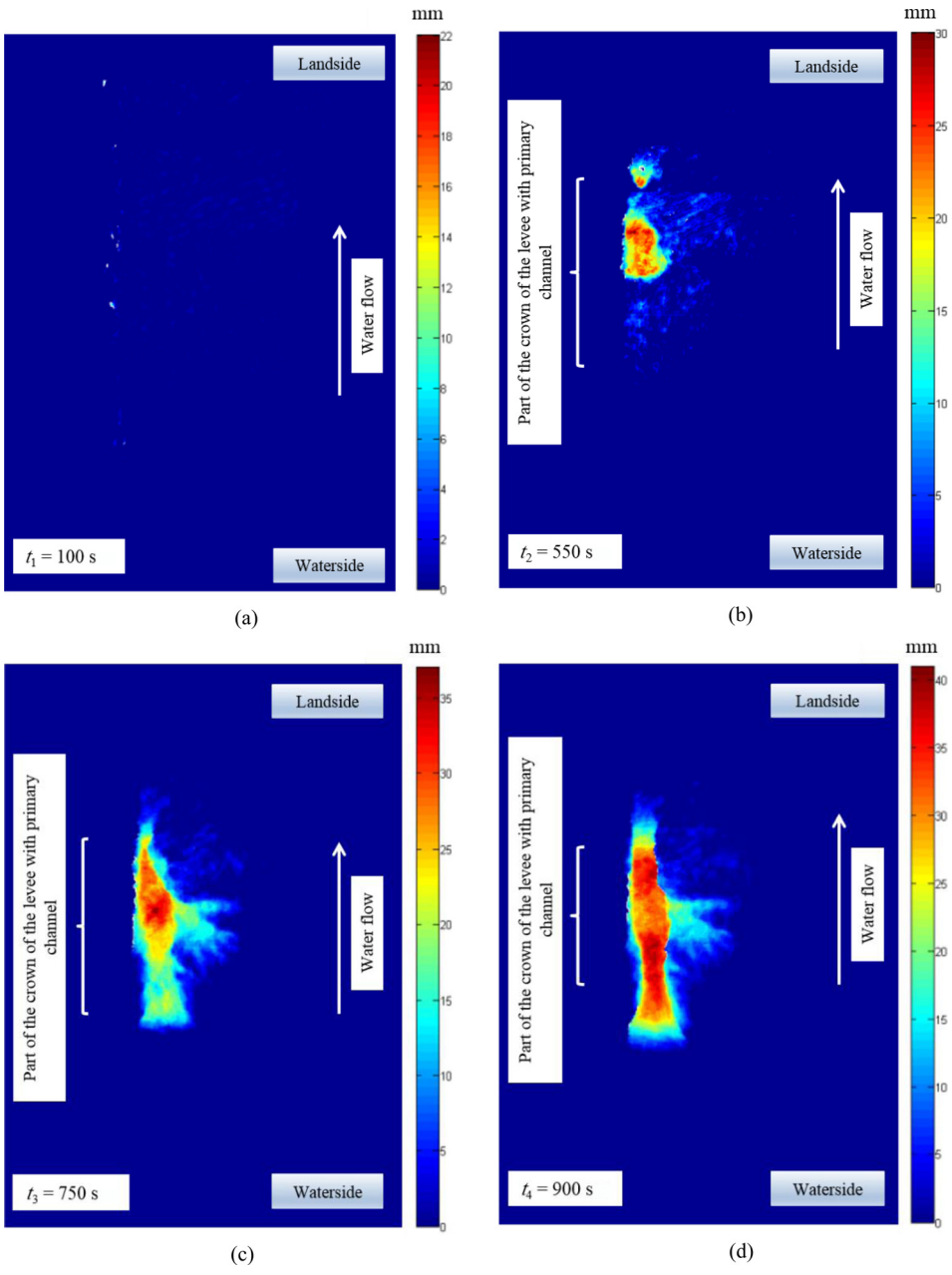

As an example, analysis of the results of one of the centrifuge experiments (experiment CMBL-04) that was also performed on frames recorded prior to formation of the primary channel is presented in **Fig. 15(a)–15(d)**. The formation of the primary channel can be clearly seen in this figure. These results were obtained after reducing the noise from the raw data, and cropping the main channel from the image. The volume of the channel for each of the images was also calculated. Three-dimensional figures could also be obtained from different viewing angles at differing times.

To investigate the variation of the depth of the main channel along its path, elevation maps were also produced. An elevation view of the primary channel after full breach for the same experiment shown in **Fig. 15** (experiment CMBL-04) is presented in **Fig. 16**. This kind of channel mapping can be helpful for validating computer simulations.

The erosion data in this study can be obtained by using other methods, for example, laser and other more sophisticated technology, which are generally expensive and time consuming. The use of the Kinect device, a low-cost, virtually throw-away sensor, is a practical and economical method to obtain quite accurate erosion data. Most importantly, in this project, it enabled the acquisition of the rate of erosion.

J_ID: GTJ DOI: 10.1520/GTJ20140226 Date: 25-January-16 Stage: Page: 14 Total Pages: 17

FIG. 16

Elevation view of the primary channel after full breach for experiment CMBL-04.

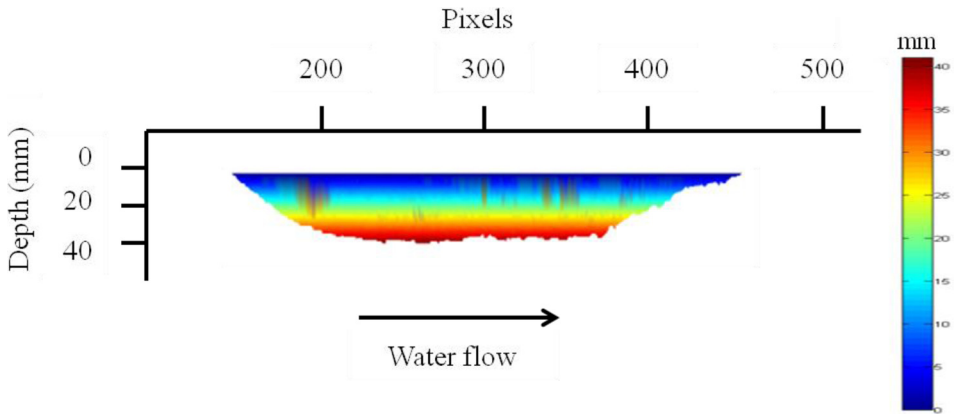

Other Applications

The use of the Kinect sensor was also investigated in other laboratory experiments. The surfaces of a series of centrifuge experiments performed at Rensselaer Polytechnic Institute have been scanned with the Kinect. These experiments were performed to study the effects of surface explosions on embankments dams, levees, and pipelines (De et al. 2013). The centrifuge tests were performed using relatively high *g*'s (80–100 *g*'s) modeling large prototype structures. The explosions occurred while the centrifuge was spinning. After an explosion, the dimensions and volume of the crater were measured. Various methods can be used, such as plaster impressions, laser scans, or physical depth measurements point by point; however, these methods tend to be time consuming, and the Kinect sensor was utilized as an alternative.

Four different experiments were scanned with Kinect in addition to other conventional measurement methods. To calculate the volume of the crater, the surface of each model was scanned prior to the experiment, and after completion of the experiment. **Fig. 17(a)** and **17(b)** shows the scanned surface of one the experiments before and after the explosion, while **Fig. 17(c)** shows the experiment setup and the location of the Kinect regarding the model box. The measured difference between these two frames would be equal to the amount of displaced soil, which would be same as the volume of the crater.

Because the shape of the crater remained constant with time, only a few frames were required to be recorded, and the scanning of the models was performed quickly. The computer codes used for the erosion data were used to analyze the scanned data. **Fig. 18(a)** shows the results of the analyses of the data after noise elimination and cropping of irrelevant scanned objects for the model shown in **Fig. 17**. Three-dimensional views of the experiment are also presented in **Fig. 18(b)**. Elevation maps were also obtained from different viewing angles for all the experiments.

The only relevant region of the model requiring scanning is the crater. The borders of the crater were clearly observed in the scanned images. Therefore, in the process of noise reduction, the coordination of the border of the crater was read manually for each experiment from the scanned images, and was set in the computer code. The computer code then cropped the image and produced 3D images. The craters volumes obtained from the Kinect data were also compared to the volumes calculated by other methods, and the results agreed well. The volume of the blast craters were determined independently by using plaster casts, metal rods in a grid pattern, and the Kinect device, and the values agreed within less than 10 %.

Conclusion

The use of a Kinect sensor, a relatively inexpensive, almost throw-away sensor, provided a practical method to determine the quantity and rate of erosion with good precision. Information about the variation of channels' shape and volume can be acquired at different times. The pattern of the propagation of the initial rills along with the information regarding depth and volume can also be recorded over time. In typical laboratory erosion experiments, initial conditions and final conditions are usually determined, but it is difficult to measure sediment volumes and erosion rates during the conduct of the experiments. This can be rapidly and economically accomplished using the Kinect device. The following specific conclusions can be drawn from the study:

1. The data produced over the course of this research validated the behavior predicted by the numerical models. Although the process of channel formation during an overtopping experiment was recorded with conventional methods, the Kinect sensor was used as a new methodology to measure and evaluate soil transportation in the erosion experiments.

J_ID: GTJ DOI: 10.1520/GTJ20140226 Date: 25-January-16 Stage: Page: 15 Total Pages: 17

FIG. 17 Scanning the surface of one the explosion experiments (a) scanned surface before the explosion, (b) scanned surface after the explosion, and (c) the experiment setup.

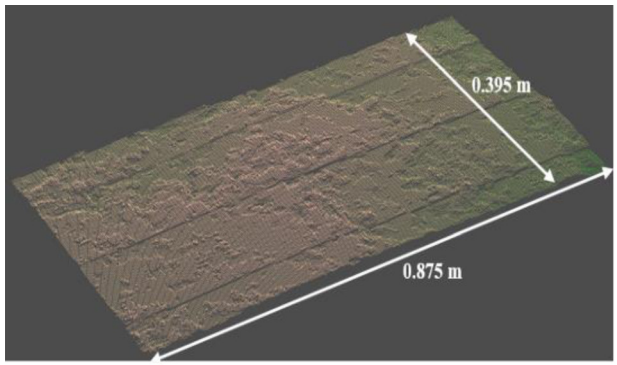

(a)

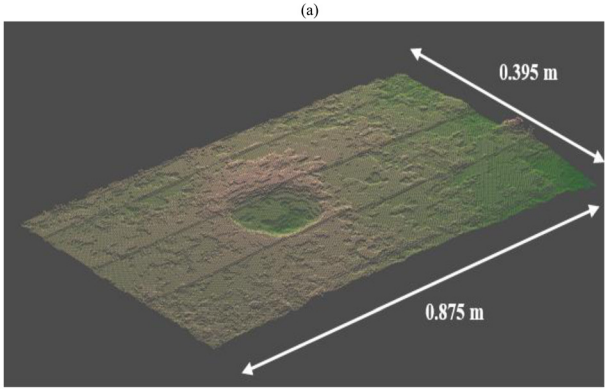

(b)

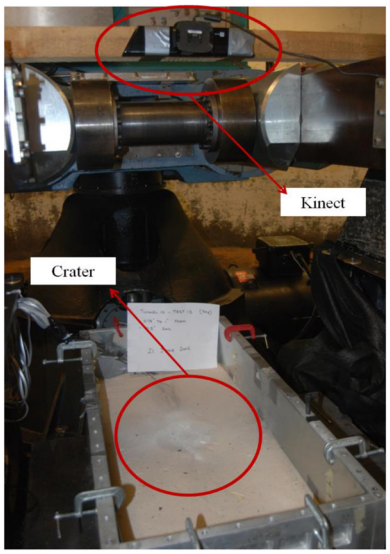

(c)

FIG. 18 Results of the analyses of the data after noise reduction and cropping irrelevant scanned objects (a) plan view of the crater after explosion experiment, and (b) three-dimensional view of the crater after explosion experiment.

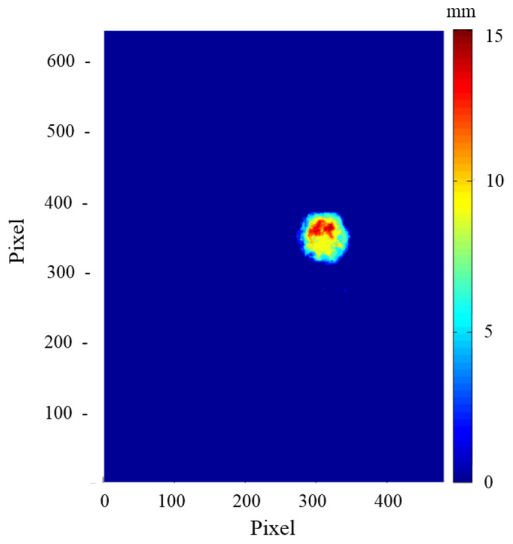

(a)

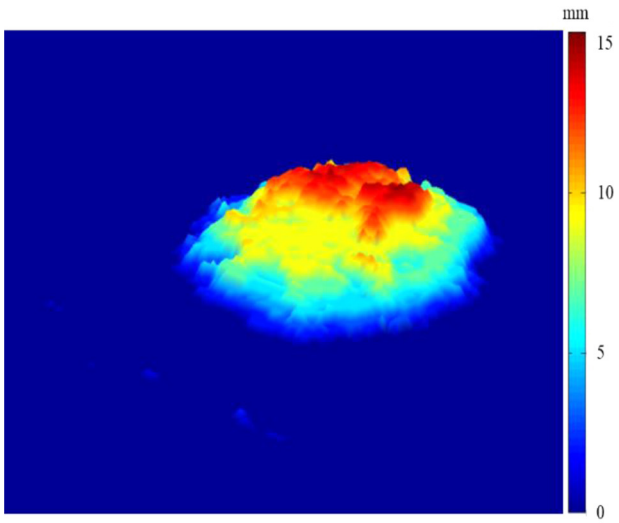

(b)

2. The new visualization methodology not only makes it feasible to record the precise duration of different erosion phases, but also to measure erosion quantity and calculate the volume of eroded soil in an erosion experiment. To the authors' knowledge, this is the first time that the methodology has been applied to the study of soil erosion.
3. Unlike a regular camera or even a high-speed camera, the Kinect records additional information regarding elevations and depths of different parts of the channels. The variations of shape and volume of the eroded channels could be measured as a function of time during the experiments, and the rate of sediment transport can be calculated.
4. Centrifuge tests were also performed to simulate real (prototype) size levees, and the application of this methodology was also studied in centrifuge testing.
5. The Kinect functioned well in 1*g* experiments and at high *g* levels in the centrifuge tests. It is believed that this is the first use of a Kinect device in centrifuge experiments. The application of the Kinect sensor in other laboratory experiments is also presented.

ACKNOWLEDGMENTS

This material is based on work supported by the National Science Foundation under Grant No. 0835762 and Grant IIS-1117277 and the Civil and Environmental Engineering Department at Rensselaer Polytechnic Institute.

References

Andrawes, K. Z. and Butterfield, R., 1973, "The Measurement of Planar Displacements of Sand Grains," *Geotechnique*, Vol. 23, No. 5, pp. 571–576.

ASTM D6913-04-e1, 2009: Standard Test Methods for Particle-Size Distribution (Gradation) of Soils Using Sieve Analysis, ASTM International, West Conshohocken, PA, www.astm.org

Briaud, J. L., Chen, H. C., Govindasamy, A. V., and Storesund, R., 2008, "Levee Erosion by Overtopping in New Orleans During the Katrina Hurricane," *J. Geotech. Geoenviron. Eng.*, Vol. 134, No. 5, pp. 618–632.

Butterfield, R., Harkness, R. M., and Andrawes, K. Z., 1970, "A Stereo-Photogrammetric Technique for Measuring Displacement Fields," *Geotechnique*, Vol. 20, No. 3, pp. 308–314.

De, A., Butler, S., and Zimmie, T., 2013, "Effects of Surface Explosions on Top of Earth Embankment Dams," *Proceedings of the Geo-Congress 2013: Stability and Performance of Slopes and Embankments III*, San Diego, CA, Mar 2013, pp. 444–447.

Dean, R. G., Rosati, J. D., Walton, T. L., and Edge, B. L., 2010, "Erosional Equivalences of Levees Steady and Intermittent Wave Overtopping," *Ocean Eng.*, Vol. 37, No. 1, pp. 104–113.

Dong, W. and Selvadurai, A. P. S., 2006, "Image Processing Technique for Determining the Concentration of a Chemical in a Fluid-Saturated Porous Medium," *Geotech. Test. J.*, Vol. 29, No. 5.

Gingold, R. A. and Monaghan, J. J., 1977, "Smoothed Particle Hydrodynamics: Theory and Application to Non-Spherical Stars," *Mon. Not. R. Astron. Soc.*, Vol. 181, No. 3, pp. 375–389.

Goyer, G. G. and Watson, R., 1963, "The Laser and Its Application to Meteorology," *Bull. Am. Meteorol. Soc.*, Vol. 44, No. 9, pp. 564–575.

Holmes, D. W., Williams, J. R., and Tilke, P., 2011, "Smooth Particle Hydrodynamics Simulations of Low Reynolds Number Flows Through Porous Media," *Int. J. Numer. Anal. Methods Geomech.*, Vol. 35, No. 4, pp. 419–437.

Iskander, M. G., Lai, J., Oswald, C. J., and Mannheimer, R. J., 1994, "Development of a Transparent Material to Model the Geotechnical Properties of Soils," *Geotech. Testing J.*, Vol. 17, No. 4.

Kamalzare, M., 2013, "Investigation of Levee Failure because of Overtopping and Validation of Erosion Evolution and Quantity," PhD dissertation, Department of Civil and Environmental Engineering, Rensselaer Polytechnic Institute, Troy, NY.

Kamalzare, M., Chen, Z., Stuetzle, C., Cutler, B., Franklin, W. R., and Zimmie, T. F., 2011, "Computer Simulation of Overtopping of Levees," *14th Pan-American Conference on Soil Mechanics and Geotechnical Engineering (64th Canadian Geotechnical Conference)*, The Canadian Geotechnical Society, Toronto, Ontario, Canada.

Kamalzare, M., Stuetzle, C., Chen, Z., Zimmie, T. F., Cutler, B., and Franklin, W. R., 2012a, "Validation of Erosion Modeling: Physical and Numerical," *Geo-Congress*, Oakland, CA, Mar 25–29, pp. 710–719.

Kamalzare, M., Zimmie, T. F., Stuetzle, C., Cutler, B., and Franklin, W. R., 2012b, "Computer Simulation of Levee's Erosion and Overtopping," *XII International Symposium on Environmental Geotechnology, Energy and Global Sustainable Development*, International Society for Environmental Geotechnology, Los Angeles, CA, June 27–29, pp. 264–273.

Kamalzare, M., Han, T. S., McMullan, M., Stuetzle, C., Zimmie, T., Cutler, B., and Franklin, W. R., 2013a, "Computer Simulation of Levee Erosion and Overtopping," *Proceedings of the Geo-Congress 2013: Stability and Performance of Slopes and Embankments III*, San Diego, CA, Mar 3–7, pp. 1851–1860.

Kamalzare, M., Zimmie, T. F., Han, T. S., McMullan, M., Cutler, B., and Franklin, W. R., 2013b, "Computer Simulation of Levee's Erosion and Overtopping," *Proceedings of the 18th International Conference on Soil Mechanics and Geotechnical Engineering (ICSMGE)*, Paris, France, Sept 2–6

Lo, H. Ch., Tabe, K., Iskander, M., and Yoon, S. H., 2010, "A Transparent Water-Based Polymer for Simulating Multiphase Flow," *Geotech. Test. J.*, Vol. 33, No. 1, pp. 1–13.

Pan, B., Qian, K., Xie, H., and Asundi, A., 2009, "Two-Dimensional Digital Image Correlation for In-Plane Displacement and Strain Measurement: A Review," *Meas. Sci. Technol.*, Vol. 20, No. 6

Raffel, M., Willert, C., Wereley, S., and Kompenhaus, J., 2007, *Particle Image Velocimetry—A Practical Guide*, Springer, Berlin.

Raschke, S. A. and Hryciw, R. D., 1997, "Grain-Size Distribution of Granular Soils by Computer Vision," *Geotech. Testing J.*, Vol. 20, No. 4.

Stanier, S. A. and White, D. J., 2013, "Improved Image-Based Deformation Measurement in the Centrifuge Environment," *Geotech. Testing J.*, Vol. 36, No. 6, pp. 915–928.

Stuetzle, C., 2012, "Representation and Generation of Terrain Using Mathematical Modeling," PhD dissertation, Department of Computer Science, Rensselaer Polytechnic Institute, Troy, NY.

Stuetzle, C., Cutler, B., Chen, Z., Franklin, W. R., Kamalzare, M., and Zimmie, T. F., 2011, "Measuring Terrain Distances Through Extracted Channel Networks," *19th ACM SIGSPATIAL International Conference on Advances in Geographic Information Systems*, Vol. 3, No. 3, Chicago, IL, Nov 1–4, pp. 21–26.

Sutton, M. A., Oreu, J.-J., and Schreier, H. W., 2009, *Image Correlation for Shape, Motion and Deformation Measurements*, Springer, New York.

White, D. J., Take, W., and Bolton, M., 2003, "Soil Deformation Measurement Using Particle Image Velocimetry (PIV) and Photogrammetry," *Geotechnique*, Vol. 53, No. 7, pp. 619–631.

Xiao, H., Huang, W., and Tao, J., 2009, "Numerical Modeling of Wave Overtopping a Levee During Hurricane Katrina," *Comput. Fluids*, Vol. 38, No. 5, pp. 991–996.

Yu, M., Deng, Y., Qin, L., Wang, D., and Chen, Y., 2009, "Numerical Simulation of Levee Breach Flows Under Complex Boundary Conditions," *J. Hydrodyn.*, Vol. 21, No. 5, pp. 633–639.